

DEUTSCHES ELEKTRONEN-SYNCHROTRON

DESY 93-109
July 1993



Partons and QCD Effects in the Pomeron

G. Ingelman

Deutsches Elektronen-Synchrotron DESY, Hamburg

and

Dept. of Radiation Sciences, Uppsala University, Sweden

ISSN 0418-9833

NOTKESTRASSE 85 - 22603 HAMBURG

DESY behält sich alle Rechte für den Fall der Schutzrechtserteilung und für die wirtschaftliche Verwertung der in diesem Bericht enthaltenen Informationen vor.

DESY reserves all rights for commercial use of information included in this report, especially in case of filing application for or grant of patents

To be sure that your preprints are promptly included in the
HIGH ENERGY PHYSICS INDEX,
send them to (if possible by air mail):

**DESY
Bibliothek
Notkestraße 85
22603 Hamburg
Germany**

**DESY-IfH
Bibliothek
Platanenallee 6
15738 Zeuthen
Germany**

Partons and QCD Effects in the Pomerom

G. Ingelman

Deutsches Elektronen-Synchrotron DESY, Notkestrasse 85, D-22607 Hamburg, FRG
Dept. of Radiation Sciences, Uppsala University, Box 535, S-751 21 Uppsala, Sweden

Abstract. The quark and gluon content of the pomerom and the notion of a pomerom structure function is discussed. The pomerom is argued to be a small object and, as a consequence, small- x gluon recombination effects could be sizeable. Ways to measure the pomerom parton densities in $p\bar{p}$ and $e\bar{p}$ collisions are presented.

1 Introduction

Diffractive scattering involves the exchange of energy-momentum but no quantum numbers and is described in terms of pomerom (P) exchange [1]. Although Fegge theory provides a useful formalism it has not led to a sufficient understanding of the pomerom and its interaction mechanism. In a modern QCD language it is natural to consider the strongly interacting pomerom as a partonic system [2] which can be probed in hard scattering processes [3]. By assuming the pomerom to behave essentially as a hadron and introducing the concept of a pomerom structure function [3] it is possible to calculate the cross-section for various diffractive hard scattering processes in pomerom-hadron and pomerom-lepton collisions [3-6] and to simulate the resulting hadronic final states [7, 8]. From this one can deduce important features that are characteristic for different ideas about the pomerom structure, but the details are uncertain due to the lack of theoretical understanding and experimental information. These issues will be discussed in the following with emphasis on the question of quark or gluon dominance in the pomerom (section 2), the pomerom size (section 3), gluon recombination effects (section 4), probing the pomerom structure function in deep inelastic scattering (DIS) at HERA (section 5), and, finally some concluding remarks.

2 Quarks or gluons in the pomerom?

The main experimental result is the clear observation of diffractive hard scattering phenomena through the discovery of high- p_T jets in diffractively excited high mass states in $p\bar{p}$ collisions at CERN [9]. This signals hard parton level scattering in the pomerom-proton collision and, furthermore, a hard parton distribution in the pomerom is advocated [10]. These data do not, however, allow a discrimination between a quark and gluon content in the pomerom. The reported diffractive production of bottom mesons by UA1 [11], which would receive a dominant contribution from the subprocess $gg \rightarrow b\bar{b}$, hints at a substantial gluon content with a soft momentum distribution in the pomerom but could hardly be explained by a quark-dominated pomerom [8].

The old suggestion [2] that the pomerom is mainly composed of gluons has been a common assumption. This has some experimental support [12] from double pomeron exchange (DPE) processes where the production of $f_2(1270)$ and $f_2(1720)$, which may have glueball components in their wave functions, indicates a gluon-rich environment in pomerom-pomerom collisions. The thought that diffractive scattering occurs through the exchange of a (virtual) glueball may have some theoretical support since the glueball trajectory, obtained from estimated glueball masses, has been claimed to coincide with that of the pomerom [13].

The pomerom structure function has also been investigated theoretically. In an analysis based on Regge theory a gluon-dominated pomerom was advocated and its gluon structure function discussed [4]. An attempt to derive the pomerom gluon density distribution based on QCD ladder diagrams has been made resulting in a rather soft gluon distribution function [14]. However, in an alternative approach [15] the pomerom is argued to couple in an effectively pointlike way to single quarks (similar to a photon) and its structure function dominated by a quark antiquark component (in analogy with the photon structure function) with a rather hard momentum distribution.

To obtain more information one should consider processes that require either a quark or gluon component in the pomerom. Numerical predictions may be obtained by assuring alternative forms of the pomerom structure function, e.g.

$$x f_{g/P}(x) = 6(1-x)^5, \quad x f_{g/F}(x) = 6x(1-x), \quad x f_{q/P}(x) = \frac{6}{4}x(1-x) \quad (1)$$

The first two cases correspond to a pomerom dominated by many soft gluons ($P = SG$ model) or a few hard ones ($P = HG$ model), respectively, whereas the last case corresponds to a pomerom composed essentially of a quark-antiquark pair ($P = q\bar{q}$ model). Whereas the first function has some support from the evidence for diffractive heavy flavour production [11], the latter two are more compatible with the observed diffractive jet production [10]. Concluding a 'flux' of pomerons with such pomerom parton densities and a hard parton level scattering cross section will give predictions for testable cross sections [3-8].

Since heavy flavour production at colliders is dominated by the gluon fusion process $gg \rightarrow Q\bar{Q}$ (and $gq \rightarrow g\bar{Q}\bar{q}$), one may use diffractive charm and bottom production in hadron collisions to gauge the gluon content in the pomerom [8]. On the other hand, W and Z production in single diffractive $p\bar{p}$ events at collider energies can to leading order only occur based on a quark component in the pomerom. The dominant process is $q\bar{q} \rightarrow W/Z$, whereas gluon induced interactions can only occur through suppressed higher order processes ($gq \rightarrow q + W/Z$). These diffractive W/Z production processes have been calculated [16] based on the pomerom models corresponding to eq. (1) and demonstrated to yield observably large cross sections at the Tevatron. The difference between a quark- and gluon-dominated pomerom, as shown in Fig. 1a, is encouragingly large. Due to the uncertainties in the models it is, however, not trivial to draw a firm conclusion from an observed rate of W/Z production alone.

The x -shape of the pomerom structure function can, furthermore, be obtained in diffractive Z production [16]. In the pomerom-proton collision, with cms energy $\sqrt{s_{Fp}}$, one has for the process $q\bar{q} \rightarrow Z \rightarrow \mu^+ \mu^-$ the relations $\tau = x_1 x_2 = \hat{s}/s_{Fp} = (p_3 \cdot p_4)^2/s_{Fp} = M_Z^2/s_{Fp}$ and $x_F = x_1 - x_2 = 2(p_3 \parallel + p_4 \parallel)/\sqrt{s_{Fp}}$ where p_3, p_4 are the four-momenta of the final muons. Solving for the incoming parton momentum fractions gives $x_{1,2} = (\pm x_F + \sqrt{x_F^2 + 4\tau})/2$. Applying this method on muons obtained in a Monte Carlo event simulation [16] based on the

$P = q\bar{q}$ model gives the result in Fig. 1b. The input pomeron (and proton) structure function is well reproduced and the statistical precision high enough for this kind of measurement to test a $q\bar{q}$ -model of the pomeron.

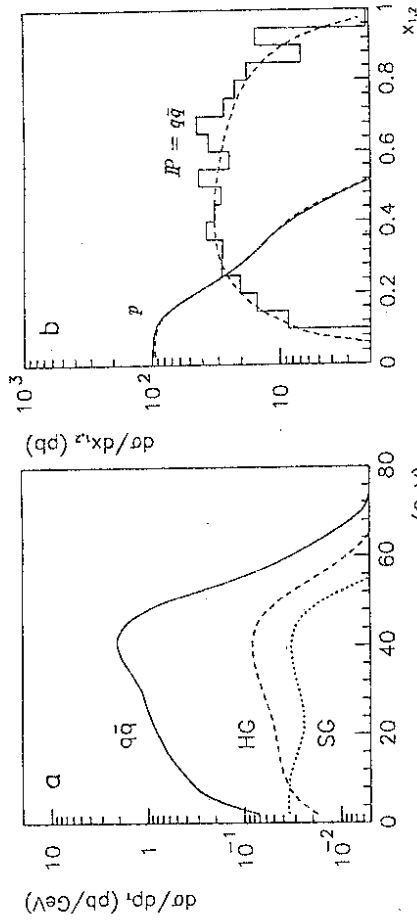


Figure 1: Diffractive production of Z -boons in $p\bar{p}$ collisions at $\sqrt{s} = 1.8 \text{ TeV}$ as obtained [16] from different pomeron models: $P = q\bar{q}$ (full), $P = \text{soft}$ gluons (dashed), $P = \text{hard}$ gluons (dotted), $P = g\bar{g}$ (dotted). (a) Distributions of transverse momentum of decay muons ($Z \rightarrow \mu^+ \mu^-$). (b) Distributions of the momentum fractions x_1, x_2 for the interacting partons in the pomeron and proton, respectively. The curves/histogram correspond to the distributions used as input (dashed) and obtained through the reconstruction (full) from $Z \rightarrow \mu^+ \mu^-$; the histogram illustrates the statistical precision with 10 pb^{-1} .

A main uncertainty for this kind of calculations is the unknown pomeron structure function. The normalisation in eq. (1) is determined by the momentum sum rule

$$\int_0^1 dx x f(x) = 1 \quad (2)$$

This is a natural choice that have commonly been used and also theoretically motivated [4]. However, the sum rule is not saturated in the model [15] where the pomeron behaves similar to a photon, with an effectively pointlike coupling to quarks, resulting in $x f_{q/P}(x) \approx 0.2x(1-x)$.

3 The pomeron size

There are reasons to believe that the pomeron is a smaller object than a normal hadron. Although there is no well defined strong interaction radius of a hadron, one may use an optical model and relate its total cross-section to its radius via $\sigma \sim \pi R^2$. This approach was used in [6] to estimate the pomeron radius from various pomeron cross sections obtained based on the factorisation between different pomeron vertices. Single diffraction data gives a pomeron-proton total cross section of about 1 mb , i.e. much smaller than a typical hadron-proton cross-section. The analysis is simplified if two identical particles are considered and

one should therefore consider the pomeron-pomeron total cross-section σ_{PP} . This can be obtained from data on double pomeron exchange (DPE) processes or from the triple pomeron vertex which in Regge theory is related to the single diffractive cross section. Consistent results are obtained in the interval $\sigma_{PP} = 0.1 \dots 0.3 \text{ } \mu\text{b}$ which lead to a pomeron radius of $R_P \approx 0.1 \text{ fm}$. Since this is obtained by comparing with the proton-proton total cross section it depends on the assumption that the pomeron has the same ‘blackness’ as the proton, which introduces an uncertainty in that a small pomeron cross section may partly result from a larger ‘transparency’ and not only from a smaller size. The value is, however, in reasonable agreement with the value 0.17 fm obtained from exclusive ρ -production in DIS [17].

Further evidence for a small pomeron can be obtained from a recent QCD sum rule calculation of the gluon form factor in the proton [18]. The resulting radius $0.3 \dots 0.35 \text{ fm}$ of the gluon system is considerably smaller than the proton radius. It is reasonable to relate this size also with the pomeron, in particular when considering the QCD gluon ladder diagram representation of the pomeron [14].

4 Gluon recombination in the pomeron

If the pomeron is essentially a gluonic object (glueball) of small size it gives the possibility to study gluon dynamics at high densities. In such an environment QCD predicts the occurrence of gluon recombination, i.e. the process $gg \rightarrow g$. This new phenomenon, which has not yet been observed, leads to a reduction of the gluon density as compared to the conventional GLAP evolution where only splittings (e.g. $g \rightarrow gg$) occur. The recombination is incorporated in the GLR equation [19] based on multi-ladder or ‘fan’ diagrams in QCD. This equation considers only pure gluon dynamics, which should dominate at small x and is particularly applicable to the pomeron, but is difficult to use numerically. A more convenient form for the gluon density evolution (but without the parton transverse momentum dependence as in GLR) is given by [20]

$$\frac{\partial z g(z, Q^2)}{\partial \ln Q^2} = \frac{\alpha_s(Q^2)}{2\pi} z \int_z^1 \frac{dy}{y^2} y g(y, Q^2) P_{gg} \left(\frac{z}{y} \right) - \frac{81\alpha_s^2(Q^2)}{16R^2 Q^2} \theta(y_{\max} - z) \int_z^{y_{\max}} \frac{dy}{y} [y g(y, Q^2)]^2 \quad (3)$$

i.e. the Altarelli-Parisi equation is modified by the second term due to the gluon recombination which depends on the size R of the object. Numerical estimates [21] for the inclusive proton structure function show that the recombination, or screening, effect is quite small in the HERA kinematic range and therefore hard to observe. It has been speculated [22] that the proton may contain hot spots, i.e. smaller regions with a higher than average gluon density (possibly around the valence quarks), such that an effectively smaller radius should be used resulting in a larger recombination term.

Applying eq. (3) to the pomeron [6] with $R_P = 0.1 \text{ fm}$ results in a large gluon recombination effect as shown in Fig. 2a. The starting gluon distribution at Q_0^2 is here chosen rather conservatively. A distribution which is larger at small fractional momentum z in the pomeron would give an even larger recombination term in eq. (3) due to the quadratic gluon density dependence. Although one may question the applicability of eq. (3) when the magnitude of the non-linear correction term becomes comparable to the leading linear one, it illustrates the possibility to reach high gluon densities in the pomeron resulting in the occurrence of new QCD effects. The gluon recombination effect is in any case much larger

than in the proton, even when assuming the hot spot scenario as illustrated in Fig 2b. In contrast to the proton, where gluon recombination only occurs at very small x , it occurs at larger momentum fractions in the pomeron.

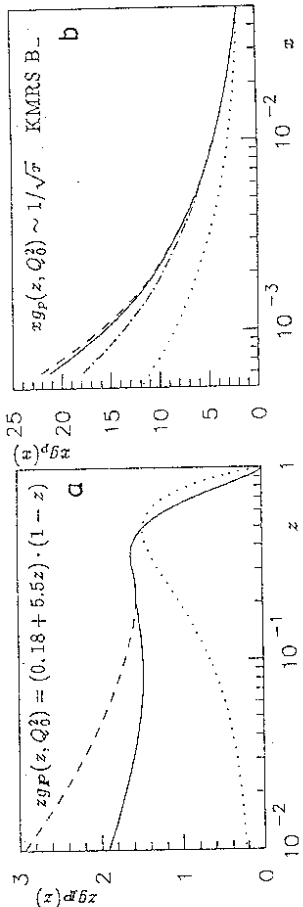


Figure 2: The gluon distributions in (a) the pomeron and (b) the proton [6]. The indicated initial distributions at $Q_0^2 = 4 \text{ GeV}^2$ (dotted curves) are evolved with QCD to $Q^2 = 50 \text{ GeV}^2$ using standard Altarelli-Parisi (dashed curves) and including the gluon recombination term (full curves), which is also applied for a hot spot dominated proton (dashed-dotted curve). The momentum fractions z and x in the pomeron and proton are related by $z = x/x_P$, where a typical pomeron momentum fraction $x_P = 0.05$ is used for comparison.

5 Probing the Pomeron in DIS

The cleanest way to probe the pomeron and measure its structure function should be provided by deep inelastic $e p$ scattering at HERA. In fact, ‘diffractive-like’ events with large rapidity gaps in the proton beam direction have already been observed [23]. With $Q^2 \gtrsim 10 \text{ GeV}^2$ this is presumably the first evidence for a genuine photon-pomeron interaction, since contributions from the photon having fluctuated into a hadronic state should then be highly suppressed.

Relying on the pomeron factorisation hypothesis, the process proceeds by the ‘emission’ of a pomeron from the proton followed by electron-pomeron DIS. Although any electroweak exchange (γ, Z, W) should be possible, we will here only consider the dominating electromagnetic cross section (neglecting $R = \sigma_L/\sigma_T$) [6]

$$\frac{d\sigma(ep \rightarrow epX)}{dx_F dt dz dQ^2} = \frac{4\pi\alpha^2}{x Q^4} \left\{ 1 - y + \frac{y^2}{2} \right\} F_2^{diff}(x, Q^2; x_F, t) \quad (4)$$

The inclusive proton structure function F_2 is here replaced by a corresponding diffractive one, F_2^{diff} , including the dependence on $x_F = 1 - P_{||}/P_{||S}$ and $t = (P_i - P_f)^2$ for the longitudinal momentum fraction and squared momentum transfer carried by the pomeron. This function can be factorized [6]

$$F_2^{diff}(x, Q^2; x_F, t) = f_{F/P}(x_F, t) F_2^P\left(\frac{x}{x_F}, Q^2\right) \quad (5)$$

into the pomeron flux (obtainable from data on diffractive scattering) and the pomeron structure function $F_2^P(z = x/x_F, Q^2) = \sum_f e_f^2 [z g_f^P(z, Q^2) + z \bar{g}_f^P(z, Q^2)]$.

If the pomeron is dominantly a gluonic object these quark distributions have to be obtained from gluon-to-quark conversion in QCD. The simple lowest order formula for the box diagram of $\gamma g \rightarrow q\bar{q}$ gives an order of magnitude estimate, whereas an improvement can be obtained by integrating the Altarelli-Parisi equation or the Mueller-Qui equation [20] which takes gluon recombination into account. However, the usual strong ordering of parton virtualities or transverse momenta may not apply at small x and a better formula is then [24]

$$F_2(z, Q^2) = \sum_f e_f^2 \int_{k_0^2}^{\infty} \frac{dk^2}{k^2} \frac{P(k^2, Q^2)}{4\pi} \frac{\alpha_s(k^2)}{\partial z g(z, k^2)} \quad (6)$$

where the dependence on the gluon virtuality k^2 is taken into account. P_2 is a generalised splitting function compared to the simple leading log case with a dependence on longitudinal momentum alone. For the derivative of the gluon distribution one can directly insert the right-hand side of eq. (3) and obtain a result for F_2^P with or without the gluon recombination term. A detailed investigation of this approach is presented in ref. [6].

The resulting expectations for $F_2^P(x, Q^2)$ are illustrated in Fig. 3. A large effect of the gluon recombination can be seen, actually relatively larger than for the gluon distribution at the same x and Q^2 due to the integration of the effect from small k^2 in eq. (6). Since the conditions used for Fig. 3 correspond to a kinematic region accessible at HERA and the error bars represent the statistical errors from about 2 months running at design luminosity with full acceptance, this demonstrates the feasibility of these measurements. Ideally, one should have the diffractive cross section in bins of x , Q^2 , x_F and t in order to fully investigate the pomeron structure function through a QCD analysis. This should give the parton densities in the pomeron and, hopefully, show a better agreement with QCD when the gluon recombination is included. The pomeron size parameter may then also be determined.

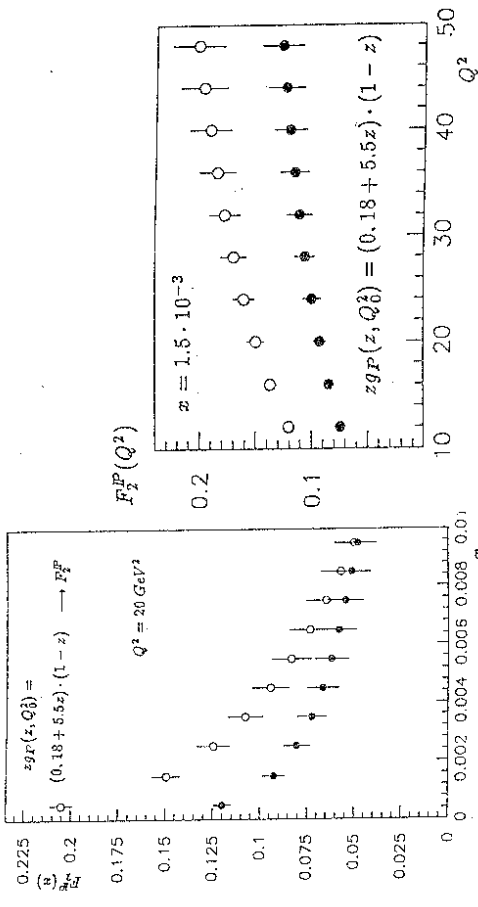


Figure 3: The dependence on x (or z since $z = x/x_F$) and Q^2 of the pomeron structure function F_2^P [6]. The specified initial gluon distribution at $Q_0^2 = 4 \text{ GeV}^2$ is evolved using Altarelli-Parisi (unfilled symbols) and including gluon recombination (filled symbols). The statistical error bars represent 10 pb^{-1} using the cross-section eq. (4) at HERA for the region $0.04 \leq x_F \leq 0.06$, $|t| \leq 0.2 \text{ GeV}^2$, $Q^2 = 20 \pm 2 \text{ GeV}^2$, $\Delta x = 0.001$.

6 Concluding remarks

A parton structure of the pomeron seems established and some information is available on the pomeron's parton distribution at rather large x . However, its behaviour at small- x is unknown and also whether it is dominated by quarks or gluons. One may question whether the normal concept of a structure function applies to a virtual object like an exchanged pomeron. To investigate this it would be interesting to do DIS at HERA on a pion, tagged through a forward neutron detector [25], since the real particle counterpart is then known.

The small pion size may then give a sizeable gluon recombination effect, although not as large as expected for the pomeron. Another question, which might be related, is the validity of factorisation, which applies in 'soft' Regge theory and has been argued [4] to hold also for diffractive hard scattering. Calculations of such processes rely on the factorisation of the cross section into a 'flux' of pomerons 'emitted' by the proton and the probability to find a parton in the pomeron. This simple concept of the pomeron structure function can, therefore, only be used if factorisation is valid and the pomeron flux is unambiguously defined. This is essentially the requirement for being able to treat the pomeron as a, more or less normal, hadronic state.

The recent UA8 result [10] of a very hard, δ -function like, component in the pomeron structure function demonstrates that essentially the whole pomeron may take part in the hard scattering process. This has been interpreted in favour of the Donnachie-Landshoff model [26], but it may also be interpreted as a coherent interaction of a gluonic pomeron [27]. This coherent interaction is argued [27] to break factorisation and become increasingly important at larger t where it co-exists with the simple non-coherent process involving a particle-like pomeron that can be described by a structure function. In electroweak diffractive scattering at large Q^2 , as accessible at HERA, the coherent part is not expected to contribute [27] and, therefore, the treatment in section 5 should then be applicable.

Although our understanding of the pomeron has improved much since the introduction of diffractive hard scattering, major problems are unsolved. As discussed, important information can be obtained through diffractive production of jets, heavy flavours and W/Z in $p\bar{p}$ colliders as well as a DIS measurement of the pomeron structure function at HERA.

Acknowledgement: I am grateful to P. Bruni and K. Pritzl for fruitful collaboration on topics reviewed here.

References

- [1] K. Goulianos, Phys. Rep. 101 (1983) 169
- [2] F.E. Low, Phys. Rev. D12 (1975) 163
S. Nussinov, Phys. Rev. Lett. 34 (1975) 1286; Phys. Rev. D14 (1976) 246
- [3] G. Ingelman, P. Schlein, Phys. Lett. 152B (1985) 256
- [4] E.L. Berger, J.C. Collins, D.E. Soper, G. Sterman, Nucl. Phys. B286 (1987) 704
- [5] H. Fritzsch, K.H. Streng, Phys. Lett. 164B (1985) 391
N. Artega-Romero, P. Kessler, J. Silva, Mod. Phys. Lett. A1 (1986) 211
K.H. Streng, in Proc. of the HERA Workshop, Hamburg 1987, Ed. R.D. Peccei (DFSY)
- [6] G. Ingelman, K. Pritzl, Z. Phys. C58 (1993) 285
- [7] P. Bruni, G. Ingelman, A. Solano, in Proc. 'Physics at HERA', Eds. W. Buchmüller, G. Ingelman, DESY Hamburg 1991, vol. 1, p. 363
- [8] P. Bruni, G. Ingelman, in Proc. workshop on 'Small- x and diffractive physics at the Tevatron', Fermilab, September 1992
- [9] R. Bonino et al., UA8 Collaboration, Phys. Lett. 211B (1988) 239
- [10] A. Brandt et al., UA8 collaboration, Phys. Lett. B297 (1992) 417
- [11] K. Eggert, UA1 collaboration, proc. 'Elastic and diffractive scattering' 1987, Ed. K. Gonianos, Editions Frontières 1988, p. 1
K. Wacker, proc. 7th Topical Workshop on Proton-Antiproton Collider Physics, Eds. R. Rajaei et al., World Scientific, 1988, p. 611
- [12] A. Breakstone et al., Z. Phys. C48 (1990) 569, Z. Phys. C58 (1993) 251
- [13] Yu. A. Simonov, Phys. Lett. 249B (1990) 514; Nucl. Phys. B(Proc. Suppl.) 23 (1991) 283
- [14] J. Barrios, G. Ingelman, Phys. Lett. 235B (1990) 175
- [15] A. Donnachie, P.V. Landshoff, Phys. Lett. 191B (1987) 309; Nucl. Phys. B303 (1988) 634
- [16] P. Bruni, G. Ingelman, Phys. Lett. B311 (1993) 317
- [17] A. Donnachie, P.V. Landshoff, Phys. Lett. 185B (1987) 403
- [18] V.M. Braun et al., Phys. Lett. B302 (1993) 291
- [19] L.V. Gribov, E.M. Levin, M.G. Ryskin, Phys. Rep. 100 (1983) 1
- [20] A.H. Mueller, J. Qiu, Nucl. Phys. B268 (1986) 427
- [21] J. Kwiecinski, A.D. Martin, W.J. Stirling, R.G. Roberts, Phys. Rev. D42 (1990) 3645
J. Porteles, J. Blümlein, G.A. Schuler, Z. Phys. C50 (1991) 91
- [22] E.M. Levin, M.C. Ryskin, in Proc. XVIII International Symposium on Multiparticle Dynamics, Tashkent 1987, Eds. I. Dzhurin, K. Guzamov, World Scientific, p. 515
E.M. Levin, M.G. Ryskin, Nucl. Phys. B (Proc. Suppl.) 18C (1990) 92
A. Mueller, Nucl. Phys. B (Proc. Suppl.) 18C (1990) 125
- [23] ZFUS and HI seminar at DESY, June 1993
- [24] E.M. Levin, M.G. Ryskin, Sov. J. Nucl. Phys. 53 (1991) 653
- [25] G. Levman, K. Furutani, ZEUS Note 92-197, DESY
- [26] A. Donnachie, P.V. Landshoff, Phys. Lett. B285 (1992) 172
- [27] J.C. Collins, L. Frankfurt, M. Strikman, Phys. Lett. B307 (1993) 161